HHS Public Access

Author manuscript

Int J Cardiovasc Imaging. Author manuscript; available in PMC 2018 April 07.

Published in final edited form as:

Int J Cardiovasc Imaging. 2018 January ; 34(1): 81–95. doi:10.1007/s10554-017-1179-y.

MRI use for atrial tissue characterization in Arrhythmias and for EP procedure guidance

Ehud J. Schmidt, PhD[1] and **Henry R. Halperin, MD**[1]

[1]Cardiology, Johns Hopkins University School of Medicine, Baltimore, MD 21205

Introduction

Atrial Fibrillation (AF) is one of the most common diseases, and is characterized by chaotic and uncoordinated contraction of the atrium[1]. The common electrocardiographic (ECG) manifestations of AF include the presence of irregular fibrillatory waves, which are waves that fragment spatially and give rise to fibrillatory conduction. It is estimated that there are 3 Million (M) patients in the US currently suffering from AF, with that number growing to 4 M by 2020 due to the aging of the population[2–4]. The cost of AF treatment to the US economy is estimated at $26–36B, with 460 thousand hospitalizations due to the disease each year[5]. In addition, AF is also the leading source of strokes in younger (<50 years old) patients[6, 7].

Pharmacological treatment of AF is <50% effective, and frequently results in substantial side-effects. Open surgery treatment of AF by cardiac surgeons began in the 1980s, with the discovery that electrical isolation of the pulmonary veins from the left atrium was able to restore many AF patients to sinus rhythm. Open surgery was sub-planted in the 1990s by intra-vascular, catheter-based, thermal (heating) - or cryogenic (cooling)- based ablative therapy, which was equally effective, but had fewer complications and a far shorter recovery time. Since then, catheter-based AF ablation has grown quickly, and there are now 160,000–180,000 ablative procedures performed each year in the US by trained electro-physiologists (EP).

With the growth in procedures, and the existence of a sizable reimbursement for the procedures, the commercial interest grew, with the current catheter ablation market estimated at $3B. As a result, there are several catheter companies whose main focus is on providing technology for treating AF. Indeed, one finds in the typical EP lab today a variety of very advanced equipment, such as digital X-ray systems, high-end ultrasound systems, robotic systems for manipulating catheters, a variety of ablation sources, and entire tool-sets of dedicated interventional devices.

Corresponding author: Ehud J. Schmidt, Ph.D., Department of Medicine (Cardiology), Johns Hopkins University, Traylor Rm. 928, 600 N Wolfe St., Baltimore, MD 21287, eschmi17@jhu.edu.

Disclosures:

Ehud J. Schmidt acknowledges funding from NIH U41-RR019703, NIH R03 EB013873-01A1, NIH U54HL119145, and AHA 10SDG261039.

Ehud J. Schmidt receives research funding support from E-TROTZ Inc., St. Jude Medical Inc. and Siemens Healthcare.

This review cannot address the causes of AF, the clinical manifestations of AF, nor does it address the various therapeutic options now available for treating AF. Readers interested in those aspects can consult several excellent text books on these subjects[8, 9]. This review is focused on MRI's increasing role in detecting the causes of AF and in monitoring the treatment of AF. Additionally, since we are making an effort to provide state-of-the-art coverage of this field, we also provide results that are not in current clinical practice, or that may not be sufficiently clinically proven for standard clinical practice. We will make an effort to denote these as such.

MRI's involvement with this field began in the early 2000s. It resulted initially from the desire to shorten the duration of the EP procedure. If MRI could provide anatomical information about the structure of the atrium non-invasively, it would save expensive interventional suite time and also reduce patient risk. This fueled the MRI work in the field, which later grew to provide unique information that was hard to obtain otherwise.

In recent years, the interest in MRI centers on improving the outcome of AF ablation, which today is only 60–70% effective for paroxysmal AF [10–13] (as measured by the incidence of recurrence one year post-ablation), with lower success rates of ~35% for non-paroxysmal AF[14–16]. As a result, many patients undergo two or more procedures, which dramatically increases the risk of complications. Since the major reason for AF recurrence is thought to be insufficient ablation of the sustaining electrical circuits during the procedure, MRI can potentially provide substantial help. MRI can improve the first AF procedure by improving planning, so the physician knows which regions in the atrium to focus on, or even decide which ablation procedure is the best therapeutic option. After the procedure, MRI can gage the procedure's success, by determining the ablated region's extent, so that repeat procedures will be more effective. During the procedure, MRI can monitor the delivery of thermal energy, in order to insure that sufficient energy is provided to cause tissue necrosis, while preventing damage to surrounding tissues, such as the esophagus.

This review has two parts. In part I, *Atrial Tissue classification in Arrhythmias*, we will discuss a few anatomic and physiological parameters of the left atrium that are of interest to the clinical community and demonstrate what MRI can provide in relation to these. In part II, *MRI for EP procedure guidance*, we will focus on MRI-guided mapping and ablative procedures for treating AF, and discuss the technology and clinical advances that have been made in this field.

I. Atrial Tissue classification in Arrhythmias

a. The anatomic structure of the normal and pathological left atrial and pulmonary vein wall

The anatomy of the cardiac left atrial wall and the surrounding pulmonary veins is geometrically and structurally complex (Figure 1). Its gross geometry has been provided for a long time by either CT or MRI imaging[17–19], and formed the first application of MRI to the field of Electrophysiology (EP). From the EP perspective, the thin (1–4 mm thick) muscle sleeves going between the atrium and the attached pulmonary veins are responsible for conducting electrical waves, originating in the pulmonary veins, into the atrium. The

muscle sleeves are surrounded by non-conducting fibrotic tissue and fat. Changes in the topology or characteristics of these thin sleeves, due to their replacement, or displacement, by fatty or fibrotic tissues, can change dramatically the electrical behavior of the left atrium, changing it from a media that does not support the fibrillatory waves which induce AF to one that does (or vis-a-versa). As a prime example, ablation of the points where these sleeves enter the left atrium (e.g. circumferential ablation) using radio-frequency (RF) energy, which replaces the muscle at that point with non-electrically-conducting fibrotic tissue, is a standard procedure used to isolate the left atrium in patients with atrial fibrillation, which can be effective in terminating simple manifestations of paroxysmal AF. [*Note that throughout this paper, we use the notation RF to designate the 500 KHz RadioFrequency thermal ablative method, whereas rf refers to the MRI radio-frequency, which is 63.8 or 123 MHz].*

More in-depth understanding of atrial wall properties is key to understanding the induction and propagation of electrical waves into the atrium[1]. Depending on the waves entering the atrium and how they propagate, normal sinus rhythm can be maintained, or abnormal paroxysmal or chronic atrial fibrillation can be observed. We briefly review this topic, since it is key to understanding both electrophysiology (EP) and the contributions (present and future) of MRI to atrial EP, since MRI may provide much of the information required for treating atrial fibrillation.

The geometry of the atria walls and the surrounding pulmonary veins, and its consequences on electrophysiology was nicely explained [20, 21], and modelled electrically to provide estimates of its consequences in supporting the rotory-shaped electrical waves (“rotors”) that create and sustain atrial fibrillation in the atria wall[22]. A major factor in understanding wave propagation is that the atrial wall is composed of a mixture of thin cardiac muscle (myocyte) sleeves, which are overlaid by fibrotic tissue and fatty tissue. The myocyte sleeves, whose shape varies within the layers of the wall, changing from the endo-cardial to the epi-cardiac surface, are highly ordered, resulting in wave propagation velocities which are also highly anisotropic. Disruption of this ordered structure, such as due to the presence of regions of fibrotic tissue, can cause AF[23, 24]. A recent study using MRI diffusion-tensor imaging (DTI) [25] of ex-vivo human atria provides excellent visualization of this complex anatomy (Figure 2). While In-vivo cardiac DTI is currently difficult to perform, there are multiple groups working on making it possible.

In addition, the atrial wall is highly innervated with large (>200 neurons) nerve ganglia plexi[26], which overlay the atrial epi-cardial surface, and reside within ordered fat-pads. Some nerve ganglia act as the substrate for re-entry of electrical waves into the pulmonary vein ostia that surround the left atrium. In addition, abnormal activity of these ganglia is important for inducing AF in its early stages, since they play an important role in regulating electrical activity[27, 28]. As a result, there are several EP groups that also ablate these ganglia plexi, although finding them using electrical methods is a lengthy procedure. [Note: ablation of the nerve ganglia is controversial in the Electrophysiology community]. MRI imaging of these mm-size nerve ganglia is now becoming possible[29], which may allow for RF ablation, which uses 500 KHz electric pulses between electrodes to ablate, or allow for cryogenic

ablation ((cryo), which uses the gas Joule-Thompson effect to cool tissues to below −40 Celsius, of atrial arrhythmia, possibly resulting in a reduced recurrence rate[30].

During the remodeling of the atrium which is caused by AF, additional fibrotic tissue is created ("AF begets AF")[31–33]. As a result, knowledge of the distribution of fibrosis in the atria can be important for understanding the propagation of fibrillatory waves[34] on the atrial wall, as well as for triaging AF therapeutic directions, such as determining which sites to ablate, or weighing the benefits of ablation versus pharmacological treatment[35]. MRI has become the prime tool for providing fibrosis information, utilizing the late gadolinium enhancement (LGE) imaging sequence[35, 36] (Figure 3), which is acquired with both ECG and respiratory synchronization in order to obtain the very high spatial resolution required for left atrial imaging.

b. What MRI visualizes in the atrium and which MRI contrasts are utilized

In the mid-1990s, MRI's utilization for pre-operative planning of EP procedures emerged as a powerful clinical tool. The first implementations utilized single-pass (rapid contrast infusion) contrast-enhanced MR angiography (CE-MRA), which provided an anatomic map of atrial anatomy. Initially, CE-MRA was performed during breath-holding and without ECG gating, which allowed for rapid acquisitions (<10 seconds), although the atrial shape obtained can be blurred, since atrial shapes can vary greatly over the cardiac cycle >40%. At a later stage, cardiac gating was added, typically together with respiratory-synchronization (navigator-echo), since navigated scans require longer scan times, which allows for obtaining higher spatial resolution. These longer acquisitions are preferably performed with a slow infusion of contrast, so that the concentration of contrast remains stable through the longer acquisition (typically 2–5 minutes). There remains significant competition between MRI and contrast-enhanced CT in providing this geometric atrial information, with CT sometimes promoted as the faster and more robust-imaging modality, especially for patients with irregular breathing and heart rate, although CT requires injection of a more nephrotoxic contrast than MRI does. For patients with frequent ectopic (PVCs or arrhythmic) beats, MRI imaging may require treatment of the arrhythmias prior to imaging, so that the patients are in sinus rhythm during imaging.

The next important contribution to pre-operative EP planning arrived with respiratory-navigated LGE. Using LGE, it became possible to observe the fibrotic tissue distribution in the atrial wall, which was information that could not easily be obtained from CT[37, 38]. Since the atrial wall is thin, typically $1mm^3$ spatial resolution LGE scans are required, which requires a high-degree of motion compensation, especially since LGE is a low Signal-to-Noise Ratio (SNR) imaging method.

EP labs that are connected with centers that have MRI scanners are frequently provided with both MRA and LGE maps prior to initiation of an EP procedure[39–42]. Atrial LGE maps are used in the EP lab to determine if and what pattern of RF ablation is required. This is important when triaging the type of RF ablation procedure required, especially when patients present with more complex and advanced AF, such as chronic AF, which may require ablating multiple locations within the atrium. Alternatively, in some centers it may be decided not to perform an ablation if the fibrosis is sufficiently extensive. LGE maps are

also useful in treating patients that have undergone prior AF ablations, with AF recurring post-procedurally, which occurs in 30–40% of paroxysmal AF patients. In such patients, the LGE (or scar) map demonstrates to the clinician the shortcomings of the prior ablations, such as the location of spatial gaps or non-transmural lesions in the ablation lines, facilitating repair of the prior work[43–45] (Figure 4) which prevents recurrence post-procedure. Repeat ablations using such MRI information have proven to be highly effective, with a very low level of recurrences. [Note that current performance of Atrial LGE requires MRI scanners with newer software versions and a high degree of MRI expertise].

Similar inter-tissue contrast (hyper-enhanced ablation lesions) to that obtained from LGE can also obtained without the use of gadolinium-based contrast agents, by use of either respiratory-navigated T1-weighted imaging[46–48], since scar tissue have a shorter T1, or respiratory-navigated multiple-cardiac-phase strain imaging, since scar or increased fibrosis reduces the elasticity of atrial tissue[49, 50], although the SNR of these sequences is typically lower than LGE. It has also recently become possible to use motion-tracking post-processing (a method borrowed from cardiac ultrasound) of retrospectively-gated multiple-cardiac-phase balanced Steady State Free Precession (cine) imaging to obtain strain images of the atrium[51, 52], although the spatial resolution of these images is lower than obtained with the traditional MRI methods used to acquire strain (DENSE, HARP, or phase-contrast).

In the future, MRI elastography, which provides a map of the shear modulus, may provide information superior to that offered by LGE. For interventional use, combining MRI elastography imaging together with Ultrasound-based excitation (Acoustic Radiation Force Imaging) may be highly valuable[53–55], since today's strain imaging methods rely on the heart's contraction for the mechanical driving force, and this becomes unreliable when ectopy occurs.

c. Acute post-RF-ablation changes in atrial anatomy and physiology

The discovery that MRI could provide important pre-operative EP information was a strong impetus for the EP community to attempt to use it for on-line monitoring of the radio-frequency ablation process, in order to reduce the large level of AF recurrence. This proved to be a larger challenge than originally estimated.

While LGE is a reliable tool to estimate the location and topology of chronic fibrosis, and therefore, also the chronic scar created by radio-frequency ablation, it was established that it did not play a reliable role in estimating the size of the necrotic lesion in the acute-injury phase, which can last for several hours after ablation. Ablation of atrial tissue is immediately associated with changes in perfusion, as well as increased edema and hemorrhage, and these may confound the picture when LGE imaging is performed minutes, or even hours, after EP ablation. It was found[44] that the lesion volume, as estimated from LGE scans performed immediately after ablation, frequently shrunk by 30–40% by the time the lesion became chronic, and edema had receded. This fact is highly significant, since the regions that do not die may again conduct electrical currents, and are thought to be one of the main reasons for AF recurrence post-procedurally.

The first method to better assess the size of the necrotic lesion in the acute phase was provided by observing lack of contrast perfusion (“no-reflow”) into the ablated zone in the immediate aftermath (3–5 minutes) post-ablation, so “black holes” in the images were observed in recently ablated regions[56]. This provided a good indication of the regions which had been somewhat heated by the EP ablation catheter, but did not provide an accurate estimate of the size of the actual necrotic lesions (i.e. the regions which had received sufficient thermal dose to die).

An improved assessment of the actual extent of ablation was provided by T1-mapping[47, 57]. The area judged by T1 mapping to be ablated proves to be a good estimate of the chronic lesion size. An even better estimate may be provided by use of T2* mapping[58, 59], which utilizes the change in magnetic susceptibility of blood due to its heating by radio-frequency energy, wherein intra-capillary blood becomes paramagnetic, leading to a decrease in its T2* value (figure 5).

Another way to estimate the total ablated region is MRI temperature imaging, which is based on the shift of the water proton resonant frequency (PRS) with temperature. Whereas this method is widely used in other body regions to obtain high spatial-resolution temperature maps, its sensitivity to motion is large, due to its dependence on small changes in the magnetic field, so its use in the heart may be difficult, although methods have been proposed for resolving these issues[60]. Success of the PRS method in predicting the extent of RF ablation was demonstrated in the left ventricle of canine models[61], with excellent correlation to LGE and histology results. It may be much harder to implement PRS in the thin left atrium, especially since the moving (air-filled) lungs which surround the atrium change the magnetic field temporally[62], although there are current efforts to address these issues.

II. MRI for EP procedure guidance

a. Methods for pre-operative planning of EP mapping and ablation

As mentioned in the previous section, a variety of MRI contrasts can be acquired prior to an Electrophysiology diagnostic and therapeutic ablation procedure. This reduces the time spent in the operating room/interventional suite on re-obtaining this information, and provides focal-regions for the electrophysiologist regarding which parts of the wall they should contact. The latter component may sometimes be important in regions of the atrium, or proximal pulmonary veins, which are difficult to access with the EP catheter, since it allows the electrophysiologist to gage the importance of spending the additional effort required to contact these areas. The most common MRI maps used today in the conventional EP lab are the MRA and LGE (scar or fibrosis) maps.

More than 90% of the EP labs perform their interventional procedures using Electro-Anatomical Mapping (EAM) workstations provided by the commercial catheter companies, notably the CARTO system of Biosense-Webster (BW, South Diamond Bar, CA), or the Ensite-NavX system of St. Jude Medical (SJM, Minnetonka, MN). EAM systems measure the instantaneous interventional-device locations while these are being navigated. They also measure the location and electrical properties of points on the atrial walls whenever this wall

is contacted by an EP catheter, which finally produces a three-dimensional map that shows both the anatomy and the electrical voltages found on the atrial wall and the surrounding proximal pulmonary veins. To incorporate the MRI information, both vendors provide applications on their workstations[63, 64] for rapid registration of the MRI information with the frame of reference used by their EAM systems. This registration is frequently performed at the very beginning of the EP procedure, so that the MRI information can then be utilized during the EAM mapping (the diagnostic) and ablation (the therapeutic) stages of the EP intervention.

Since the patient generally lies in a somewhat different orientation on the EP table relative to their position on the MRI table, and time may have elapsed between the MRI diagnostic study and the EP intervention, these registrations generally rely on using an EP catheter to touch locations in the atrium that can also be identified on the MRI maps. In addition, non-linear (i.e. changes in size) registrations may need to be performed. This is especially true for regions close to the pulmonary veins, where the voltage-tracking method, which is extensively used by both BW and SJM for all catheter electrode localizations, excluding the tip electrode on the catheter which may rely on magnetic tracking, returns less accurate positional information due to the proximity of the lungs. In totality, such MRI-EAM registrations frequently suffer from mm-scale discrepancies, which many electrophysiologists have become accustomed to.

b. Methods for navigating catheters and other devices inside the MRI

Due to the ability of MRI contrasts to monitor the ablation process, there has been a longstanding interest in performing the EP ablation procedure inside the MRI scanner. Monitoring the ablation inside the MRI requires the ability to partially, or completely, navigate the EP catheters from the vascular entry-points to the atrium inside the MRI, to visualize the catheter while it is being manipulated inside the atrium, and to monitor the heating (or freezing) process using MRI contrasts.

While it was clear that MRA provided a vascular roadmap, which was equivalent or better than the conventional X-ray fluoroscopy maps, so that the path of the catheter from the skin entry point to the atrium was known and could be planned, it was obvious that the commercial EP toolset, comprised of catheters, sheathes and guidewires, needed to be extensively modified in order to operate in the MRI environment. Most EP devices, which are long (70–130 cm) and narrow (1–3 mm diameter) devices, and must be manipulated (advanced and torqued) from a large distance by the electrophysiologist, are largely made of (or reinforced by) metallic components, since metal provides the optimal mechanical (Young’s and torsional moduli, high yield point, non-brittle behavior) properties for these geometric dimensions. In addition, many of the devices used are deflectable devices, which means that they possess mechanical levers (generally in a handle of some form) on their proximal end that allow the distal portion (“tip”) of the device to be rotated by a large angle, relative to the shaft orientation. The principle method used for tip deflection is based on strong flat metallic wires (pull-wires).

When the metals used in the device are ferromagnetic, they cannot be used at all inside the MRI’s strong static magnetic field, since strong forces act on the device. When the metals

are highly paramagnetic, they create susceptibility artifacts which extend to far larger distances relative to their physical size, which masks anatomic regions that are close to the device, and can severely limit the device's utility. In addition, long electrically-conductive metallic devices can heat as a result of resonant electro-magnetic (EM) waves induced on the metal surface by MRI's high-frequency (typically 63.8, 123.2, or 127 MHz) radio-frequency (rf) field. This is especially true when high energy deposition MRI sequences, referred to as high specific absorption rate (SAR) sequences, are used[65, 66]. Large temperature increases close to the device can create blood coagulation or internal burns.

As a result, it was clear that much of the traditional EP toolset would have to be remade in order to work inside the MRI. The larger (>2 mm) metallic-shaft devices were replaced with plastic (or polymer) shaft devices, whereas the very thin devices, such as guidewires, were built using low-conductivity and low-susceptibility metals (nitinol)[67, 68], or were remade of plastic or fiber-glass shafts[69, 70]. In addition, the standard electrodes used on the EP catheters were replaced with higher-cost platinum or gold electrodes[71], with all high-susceptibility (stainless steel, nickel) metals removed. Finally, special methods (filtering, shielding, etc.) may need to be used to mitigate any potential heating of the catheter body or its surroundings.

The second key problem that needed to be addressed was visualizing the catheter during navigation. Conventional EP labs rely on X-ray fluoroscopy, wherein a strong contrast-to-noise (CNR) ratio exists between the navigating device and the vascular background as a result of the strong x-ray absorption of the metallic device against a background of the weak absorption of blood. In addition, an X-ray fluoroscopy image provides a sum of the absorption along a certain spatial direction, so the device can be seen, no matter what its location is along that direction, and the visualization is fast, so the X-ray projection imaging can easily keep up with a rapidly moving (due to navigation) device.

To allow MRI visualization during navigation, either passive, semi-active, or active visualization methods are employed.

Passive methods for device visualization inside MRI—If a conventional plastic MRI-compatible device, such as a catheter, is placed in the blood-vessel, the device can be resolved on an MRI image, a result of the absence of MRI signal (since there are no MRI spins inside the device) at the location of the device, relative to the signal of surrounding blood, but that is a low CNR method, and in addition, it requires that the image be obtained at the exact location of the catheter, and preferably in a plane that encompasses the majority of the catheter. Stronger CNR can be obtained if methods are used to highlight the catheter. One method is coating the device surface with a layer of MRI contrast media (e.g. Gd-DTPA or other paramagnetic materials)[72], which shortens the T1 in the blood that adjoins the device. This method is mostly employed in the thinnest of devices, such as guidewires.[69, 70]. Another method for visualizing guidewires is direct injection of diluted Gd-DTPA contrast out of the catheter's inner lumen, which is analogous to the X-ray fluoroscopy method, but which, as opposed to the X-ray case, unfortunately also has the contrast infusing surrounding tissues.

Semi-active methods for device visualization inside MRI—Another method for increasing CNR, which is more widely employed, is placing resonant MRI rf coils within the device. A popular design early-on was the “loop-less” coil[73], which was a coaxial cable that ran along the catheter shaft, with the shield of the coax removed in the most distal quarter wavelength of the catheter. These rf coils can either remain un-connected to the MRI’s receiver channels, so their signal is picked up via inductive-coupling to the surface MRI coils, or they can be connected to particular MRI receiver channels, in the same manner as diagnostic MRI coils are. When such coils receive rf excitation from the MRI’s body coil excitation, they create spatially-localized higher MRI flip angles in the vicinity of the coils, so that blood flowing around the device is highlighted, and a bright region appears in the image[74–76]. An Impressive use of a semi-active device was the development of the first MRI-compatible trans-septal needles[77, 78], which is a very important device for performance of atrial interventions, since trans-septal access, namely the puncture of the inter-atria septal wall is the most common path used by electrophysiologists to access the left atrium.

The deficiency of both passive and semi-active localization lies in the fact that they both rely on MRI imaging, as well as in that they require that slices be obtained in the plane of the device, which is tricky to ensure as the devices move within the media. In effect, there needs to be a manual or automatic method to constantly chase the device as it moves. As a result, these methods both result in relatively slow tracking speeds (up to only ~4 frames-per-second (fps)), and the spatial localization resolution is typically a few mm. Their advantage is that they are simple to technically implement, do not require special MRI sequences in order to visualize the catheter, and may be somewhat safer to employ from the perspective of rf-heating, since they generally require that fewer conductive wires reside inside the catheter.

Passive catheter visualization was employed in the mid-2000s in the human atrium by John Hopkins[79] for navigation and mapping, and lately by Leipzig[80] for both navigation and RF ablation of atrial flutter. The deficiencies in navigation speed and the inaccuracy in spatial localization of passive catheters hampered their atrial use, due to the severe requirements on localization accuracy during both navigating and ablation in the atrium. As a result, the procedures performed with passive catheters required very long times, and provided relatively low therapeutic value.

Active methods for device visualization inside MRI—Active visualization relies on placement of specific sensors at specific locations on the devices that continuously broadcast their spatial location out to dedicated detectors. With active tracking, there is no need to find the device using MRI imaging, since the location of the device is continuously tracked, which allows for much higher frame rate (10–40 fps) and more accurate (sub-mm) spatial localization of the device. The deficiency of active tracking is that it requires both dedicated sensors (e. g. hardware) and dedicated software for locating the device. The EP community is well-acquainted with active tracking, since it has long depended on two methods for active tracking of catheters placed inside the heart; magnetic-tracking and voltage-tracking. These tracking methods form the basic tools employed for EP interventions that utilize the BW and SJM workstations. In addition, additional modalities used in the EP suite, such as intra-cardiac ultrasound (ICE) as well as some of the X-ray panels, are also tracked during the intervention using the above methods.

There are two MRI-based methods for tracking devices, the MRI-profile-based ("MR-Tracking") method and the gradient-induced electric voltage ("Robin-Medical") method[81].

The MR-Tracking method is the most commonly-used method, since it is easier to implement within the constraints of the small-diameter intra-vascular devices[82–84]. It relies on small (1–3 mm diameter) rf coils, most frequently solenoidal in shape, which are added onto the shaft of the device, and connected to the MRI scanner's receivers via coaxial cables that run up the shaft of the catheter. Each of these rf coils picks up a highly-localized MRI signal from its immediate environment. By applying MRI gradients in the three spatial directions (x, y, z), complete localization of these coils can be obtained in very short scan times (50ms, or 40 fps tracking rate), and with spatial resolutions of $0.5\times0.5\times0.5$ mm^3, using a dedicated MR-Tracking pulse sequence[82]. Modification of the basic MR-Tracking sequence by the addition of phase-field-dithering[84] has made the method highly reliable for intravascular use. MR-Tracking sequences, as well as visualization tools that allow observing instantaneous catheter locations during navigation, on the background of MRA-based vascular roadmaps, are currently provided by most of the MRI vendors.

MR-Tracking was first used in animals for navigation to the left atrium, followed by RF ablation at the atrium-pulmonary-vein junctions in 2008 (Figure 6) [85, 86]. Effective heat mitigation strategies for the coaxial cables that carry the MR-Tracking signal up the catheter shaft were also developed, based on placement of transformers along each coaxial cable[87], which enabled human use of the method. MR-tracking has recently been used in human clinical trials by the Leipzig and King's College (London) groups for Atrial Flutter ablation[88, 89].

Voltage-device-tracking (VDT) is a tracking method that is widely used in conventional electrophysiology, and is utilized by both BW and SJM in their EAM workstations. VDT relies on kHz-range electric fields induced into the body using 3 orthogonal sets of surface patches, which are picked up by simple ring-shaped electrodes which are placed on the shafts of many types of interventional devices. Since VDT does not use magnetic fields, works well inside MRI scanners when the MRI gradients are not pulsing (i.e. imaging is not occurring). When the MRI gradients are pulsing, the VDT signals are corrupted. A partial solution to this issue was provided by blocking VDT reception during periods of strong gradient activity[90], which allowed use of several (although not all) MRI sequences in parallel with VDT tracking. The great advantage of VDT tracking is that it can be used both outside and inside the MRI scanner. This unique feature enables EP procedures which contain sections that must currently be (due to a lack of MR-conditional devices), or are more effectively, performed outside the MRI scanner, and which therefore require moving the patient between the MRI and the conventional EP interventional suite. VDT-guided EP mapping procedures in the atrium have been performed in animal models at both Brigham and Women's Hospital (Figure 7) and Johns Hopkins. Since VDT employs a commercial tracking method, many of the visualization tools available on the commercial workstations can be used, including rapid incorporation of images obtained with multiple MRI contrasts into the EAM frame of reference used in the EP lab.

There exist additional non-MRI-based, but MRI-compatible, tracking methods that may be used in the future for MRI-guided EP. There is currently a large effort to improve Fiber Bragg Grating (FBG) sensors, a method that utilizes periodic cuts made in thin glass fibers. A laser is shined down the fiber, and multiple reflections are then obtained from each of the cuts, allowing the calculation (using interferometry) of the deformation of each segment, and thus providing a "snake-like" picture of the shape of the device[91]. There are remaining issues with the localization accuracy, but these are currently being addressed.

Conclusions

MRI has made significant progress in assisting in the diagnosis and treatment of Atrial Fibrillation. Diagnostic MRI now provides more information on the atrium than any other imaging modality, and further advances are expected in the next few years. In addition, human MRI-guided EP ablative procedures in the left atrium, which we and others have been working on for 15 years, are now becoming a reality.

References

1. Calkins H, Brugada J, Packer DL, Cappato R, Chen SA, Crijns HJ, Damiano RJ Jr, Davies DW, Haines DE, Haissaguerre M, Iesaka Y, Jackman W, Jais P, Kottkamp H, Kuck KH, Lindsay BD, Marchlinski FE, McCarthy PM, Mont JL, Morady F, Nademanee K, Natale A, Pappone C, Prystowsky E, Raviele A, Ruskin JN, Shemin RJ. Heart Rhythm S, European Heart Rhythm A, European Cardiac Arrhythmia S, American College of C, American Heart A, Society of Thoracic S. Hrs/ehra/ecas expert consensus statement on catheter and surgical ablation of atrial fibrillation: Recommendations for personnel, policy, procedures and follow-up. A report of the heart rhythm society (hrs) task force on catheter and surgical ablation of atrial fibrillation developed in partnership with the european heart rhythm association (ehra) and the european cardiac arrhythmia society (ecas); in collaboration with the american college of cardiology (acc), american heart association (aha), and the society of thoracic surgeons (sts). Endorsed and approved by the governing bodies of the american college of cardiology, the american heart association, the european cardiac arrhythmia society, the european heart rhythm association, the society of thoracic surgeons, and the heart rhythm society. Europace : European pacing, arrhythmias, and cardiac electrophysiology : journal of the working groups on cardiac pacing, arrhythmias, and cardiac cellular electrophysiology of the European Society of Cardiology. 2007; 9:335–379.
2. Colilla S, Crow A, Petkun W, Singer DE, Simon T, Liu X. Estimates of current and future incidence and prevalence of atrial fibrillation in the u.S. Adult population. The American journal of cardiology. 2013; 112:1142–1147. [PubMed: 23831166]
3. Rodriguez CJ, Soliman EZ, Alonso A, Swett K, Okin PM, Goff DC Jr, Heckbert SR. Atrial fibrillation incidence and risk factors in relation to race-ethnicity and the population attributable fraction of atrial fibrillation risk factors: The multi-ethnic study of atherosclerosis. Annals of epidemiology. 2015; 25:71–76. 76 e71. [PubMed: 25523897]
4. Schnabel RB, Yin X, Gona P, Larson MG, Beiser AS, McManus DD, Newton-Cheh C, Lubitz SA, Magnani JW, Ellinor PT, Seshadri S, Wolf PA, Vasan RS, Benjamin EJ, Levy D. 50 year trends in atrial fibrillation prevalence, incidence, risk factors, and mortality in the framingham heart study: A cohort study. Lancet. 2015; 386:154–162. [PubMed: 25960110]
5. Kim MH, Johnston SS, Chu BC, Dalal MR, Schulman KL. Estimation of total incremental health care costs in patients with atrial fibrillation in the united states. Circulation. Cardiovascular quality and outcomes. 2011; 4:313–320. [PubMed: 21540439]
6. Takabayashi K, Hamatani Y, Yamashita Y, Takagi D, Unoki T, Ishii M, Iguchi M, Masunaga N, Ogawa H, Esato M, Chun YH, Tsuji H, Wada H, Hasegawa K, Abe M, Lip GY, Akao M. Incidence of stroke or systemic embolism in paroxysmal versus sustained atrial fibrillation: The fushimi atrial fibrillation registry. Stroke; a journal of cerebral circulation. 2015; 46:3354–3361.

7. Yiin GS, Howard DP, Paul NL, Li L, Mehta Z, Rothwell PM. Oxford Vascular S. Recent time trends in incidence, outcome and premorbid treatment of atrial fibrillation-related stroke and other embolic vascular events: A population-based study. Journal of neurology, neurosurgery, and psychiatry. 2015 Oct 20.doi: 10.1136/jnnp-2015-311947
8. Zipes, DP., Jalife, J. Cardiac electrophysiology, from cell to bedside. 6. Elsevier; 2013.
9. Josephson, ME. Josephson's clinical cardiac electrophysiology 5th edition techniques and interpretations. 2015.
10. Chao TF, Ambrose K, Tsao HM, Lin YJ, Chang SL, Lo LW, Hu YF, Tuan TC, Suenari K, Li CH, Hartono B, Chang HY, Wu TJ, Chen SA. Relationship between the chads(2) score and risk of very late recurrences after catheter ablation of paroxysmal atrial fibrillation. Heart rhythm : the official journal of the Heart Rhythm Society. 2012; 9:1185–1191.
11. Kearney K, Stephenson R, Phan K, Chan WY, Huang MY, Yan TD. A systematic review of surgical ablation versus catheter ablation for atrial fibrillation. Annals of cardiothoracic surgery. 2014; 3:15–29. [PubMed: 24516794]
12. Lin YJ, Chang SL, Lo LW, Hu YF, Suenari K, Li CH, Chao TF, Chung FP, Liao JN, Hartono B, Tso HW, Tsao HM, Huang JL, Kao T, Chen SA. A prospective, randomized comparison of modified pulmonary vein isolation versus conventional pulmonary vein isolation in patients with paroxysmal atrial fibrillation. Journal of cardiovascular electrophysiology. 2012; 23:1155–1162. [PubMed: 22702369]
13. Opolski G, Januszkiewicz L, Szczerba E, Osinska B, Rutkowski D, Kalarus Z, Kazmierczak J. Readmissions and repeat procedures after catheter ablation for atrial fibrillation. Cardiology journal. 2015; 22:630–636. [PubMed: 26100826]
14. Chang HY, Lo LW, Lin YJ, Chang SL, Hu YF, Feng AN, Yin WH, Li CH, Chao TF, Hartono B, Chung FP, Cheng CC, Lin WS, Tsao HM, Chen SA. Long-term outcome of catheter ablation in patients with atrial fibrillation originating from the superior vena cava. Journal of cardiovascular electrophysiology. 2012; 23:955–961. [PubMed: 22554079]
15. Chang HY, Lo LW, Lin YJ, Chang SL, Hu YF, Li CH, Chao TF, Chung FP, Ha TL, Singhal R, Chong E, Yin WH, Tsao HM, Hsieh MH, Chen SA. Long-term outcome of catheter ablation in patients with atrial fibrillation originating from nonpulmonary vein ectopy. Journal of cardiovascular electrophysiology. 2013; 24:250–258. [PubMed: 23210627]
16. Chao TF, Tsao HM, Lin YJ, Tsai CF, Lin WS, Chang SL, Lo LW, Hu YF, Tuan TC, Suenari K, Li CH, Hartono B, Chang HY, Ambrose K, Wu TJ, Chen SA. Clinical outcome of catheter ablation in patients with nonparoxysmal atrial fibrillation: Results of 3-year follow-up. Circulation. Arrhythmia and electrophysiology. 2012; 5:514–520. [PubMed: 22550126]
17. Mansour M, Holmvang G, Ruskin J. Role of imaging techniques in preparation for catheter ablation of atrial fibrillation. Journal of cardiovascular electrophysiology. 2004; 15:1107–1108. [PubMed: 15363090]
18. Mansour M, Holmvang G, Sosnovik D, Migrino R, Abbara S, Ruskin J, Keane D. Assessment of pulmonary vein anatomic variability by magnetic resonance imaging: Implications for catheter ablation techniques for atrial fibrillation. Journal of cardiovascular electrophysiology. 2004; 15:387–393. [PubMed: 15089984]
19. Mansour M, Refaat M, Heist EK, Mela T, Cury R, Holmvang G, Ruskin JN. Three-dimensional anatomy of the left atrium by magnetic resonance angiography: Implications for catheter ablation for atrial fibrillation. Journal of cardiovascular electrophysiology. 2006; 17:719–723. [PubMed: 16836666]
20. Ho SY, Sanchez-Quintana D, Cabrera JA, Anderson RH. Anatomy of the left atrium: Implications for radiofrequency ablation of atrial fibrillation. Journal of cardiovascular electrophysiology. 1999; 10:1525–1533. [PubMed: 10571372]
21. Ho SY, Cabrera JA, Sanchez-Quintana D. Left atrial anatomy revisited. Circulation. Arrhythmia and electrophysiology. 2012; 5:220–228. [PubMed: 22334429]
22. Spach MS, Miller WT 3rd, Dolber PC, Kootsey JM, Sommer JR, Mosher CE Jr. The functional role of structural complexities in the propagation of depolarization in the atrium of the dog. Cardiac conduction disturbances due to discontinuities of effective axial resistivity. Circulation research. 1982; 50:175–191. [PubMed: 7055853]

23. Eckstein J, Zeemering S, Linz D, Maesen B, Verheule S, van Hunnik A, Crijns H, Allessie MA, Schotten U. Transmural conduction is the predominant mechanism of breakthrough during atrial fibrillation: Evidence from simultaneous endo-epicardial high-density activation mapping. Circulation. Arrhythmia and electrophysiology. 2013; 6:334–341. [PubMed: 23512204]
24. Maesen B, Zeemering S, Afonso C, Eckstein J, Burton RA, van Hunnik A, Stuckey DJ, Tyler D, Maessen J, Grau V, Verheule S, Kohl P, Schotten U. Rearrangement of atrial bundle architecture and consequent changes in anisotropy of conduction constitute the 3-dimensional substrate for atrial fibrillation. Circulation. Arrhythmia and electrophysiology. 2013; 6:967–975. [PubMed: 23969531]
25. Pashakhanloo F, Herzka DA, Ashikaga H, Mori S, Gai N, Bluemke DA, Trayanova NA, McVeigh ER. Myofiber architecture of the human atria as revealed by submillimeter diffusion tensor imaging. Circulation. Arrhythmia and electrophysiology. 2016:9.
26. Armour JA, Murphy DA, Yuan BX, Macdonald S, Hopkins DA. Gross and microscopic anatomy of the human intrinsic cardiac nervous system. The Anatomical record. 1997; 247:289–298. [PubMed: 9026008]
27. Chen PS, Chen LS, Fishbein MC, Lin SF, Nattel S. Role of the autonomic nervous system in atrial fibrillation: Pathophysiology and therapy. Circulation research. 2014; 114:1500–1515. [PubMed: 24763467]
28. Stavrakis S, Nakagawa H, Po SS, Scherlag BJ, Lazzara R, Jackman WM. The role of the autonomic ganglia in atrial fibrillation. JACC. Clinical electrophysiology. 2015; 1:1–13. [PubMed: 26301262]
29. Schmidt EJ, Noseworthy PA, Amrmour JA, Malchano Z, VYR. Location of porcine cardiac autonomic nerve plexi with fat-suppressed mri. Journal of cardiovascular magnetic resonance : official journal of the Society for Cardiovascular Magnetic Resonance. 2006; 8:237.
30. Higuchi K, Akkaya M, Koopmann M, Blauer JJ, Burgon NS, Damal K, Ranjan R, Kholmovski E, Macleod RS, Marrouche NF. The effect of fat pad modification during ablation of atrial fibrillation: Late gadolinium enhancement mri analysis. Pacing and clinical electrophysiology : PACE. 2013; 36:467–476. [PubMed: 23356963]
31. Wijffels MC, Kirchhof CJ, Dorland R, Allessie MA. Atrial fibrillation begets atrial fibrillation. A study in awake chronically instrumented goats. Circulation. 1995; 92:1954–1968. [PubMed: 7671380]
32. Burstein B, Nattel S. Atrial fibrosis: Mechanisms and clinical relevance in atrial fibrillation. Journal of the American College of Cardiology. 2008; 51:802–809. [PubMed: 18294563]
33. Nattel S, Burstein B, Dobrev D. Atrial remodeling and atrial fibrillation: Mechanisms and implications. Circulation. Arrhythmia and electrophysiology. 2008; 1:62–73. [PubMed: 19808395]
34. McDowell KS, Zahid S, Vadakkumpadan F, Blauer J, MacLeod RS, Trayanova NA. Virtual electrophysiological study of atrial fibrillation in fibrotic remodeling. PloS one. 2015; 10:e0117110. [PubMed: 25692857]
35. Marrouche NF, Wilber D, Hindricks G, Jais P, Akoum N, Marchlinski F, Kholmovski E, Burgon N, Hu N, Mont L, Deneke T, Duytschaever M, Neumann T, Mansour M, Mahnkopf C, Herweg B, Daoud E, Wissner E, Bansmann P, Brachmann J. Association of atrial tissue fibrosis identified by delayed enhancement mri and atrial fibrillation catheter ablation: The decaaf study. JAMA : the journal of the American Medical Association. 2014; 311:498–506. [PubMed: 24496537]
36. McGann C, Akoum N, Patel A, Kholmovski E, Revelo P, Damal K, Wilson B, Cates J, Harrison A, Ranjan R, Burgon NS, Greene T, Kim D, Dibella EV, Parker D, Macleod RS, Marrouche NF. Atrial fibrillation ablation outcome is predicted by left atrial remodeling on mri. Circulation. Arrhythmia and electrophysiology. 2014; 7:23–30. [PubMed: 24363354]
37. Peters DC, Wylie JV, Hauser TH, Kissinger KV, Botnar RM, Essebag V, Josephson ME, Manning WJ. Detection of pulmonary vein and left atrial scar after catheter ablation with three-dimensional navigator-gated delayed enhancement mr imaging: Initial experience. Radiology. 2007; 243:690–695. [PubMed: 17517928]
38. Lardo AC, McVeigh ER, Jumrussirikul P, Berger RD, Calkins H, Lima J, Halperin HR. Visualization and temporal/spatial characterization of cardiac radiofrequency ablation lesions using magnetic resonance imaging. Circulation. 2000; 102:698–705. [PubMed: 10931812]

39. Reddy VY, Malchano ZJ, Holmvang G, Schmidt EJ, d'Avila A, Houghtaling C, Chan RC, Ruskin JN. Integration of cardiac magnetic resonance imaging with three-dimensional electroanatomic mapping to guide left ventricular catheter manipulation: Feasibility in a porcine model of healed myocardial infarction. Journal of the American College of Cardiology. 2004; 44:2202–2213. [PubMed: 15582319]
40. Kato R, Lickfett L, Meininger G, Dickfeld T, Wu R, Juang G, Angkeow P, LaCorte J, Bluemke D, Berger R, Halperin HR, Calkins H. Pulmonary vein anatomy in patients undergoing catheter ablation of atrial fibrillation: Lessons learned by use of magnetic resonance imaging. Circulation. 2003; 107:2004–2010. [PubMed: 12681994]
41. Dickfeld T, Calkins H, Zviman M, Meininger G, Lickfett L, Roguin A, Lardo AC, Berger R, Halperin H, Solomon SB. Stereotactic magnetic resonance guidance for anatomically targeted ablations of the fossa ovalis and the left atrium. Journal of interventional cardiac electrophysiology : an international journal of arrhythmias and pacing. 2004; 11:105–115. [PubMed: 15383773]
42. Nazarian S, Bluemke DA, Lardo AC, Zviman MM, Watkins SP, Dickfeld TL, Meininger GR, Roguin A, Calkins H, Tomaselli GF, Weiss RG, Berger RD, Lima JA, Halperin HR. Magnetic resonance assessment of the substrate for inducible ventricular tachycardia in nonischemic cardiomyopathy. Circulation. 2005; 112:2821–2825. [PubMed: 16267255]
43. Dickfeld T, Kato R, Zviman M, Lai S, Meininger G, Lardo AC, Roguin A, Blumke D, Berger R, Calkins H, Halperin H. Characterization of radiofrequency ablation lesions with gadolinium-enhanced cardiovascular magnetic resonance imaging. Journal of the American College of Cardiology. 2006; 47:370–378. [PubMed: 16412863]
44. Badger TJ, Daccarett M, Akoum NW, Adjei-Poku YA, Burgon NS, Haslam TS, Kalvaitis S, Kuppahally S, Vergara G, McMullen L, Anderson PA, Kholmovski E, MacLeod RS, Marrouche NF. Evaluation of left atrial lesions after initial and repeat atrial fibrillation ablation: Lessons learned from delayed-enhancement mri in repeat ablation procedures. Circulation. Arrhythmia and electrophysiology. 2010; 3:249–259. [PubMed: 20335558]
45. Reddy VY, Schmidt EJ, Holmvang G, Fung M. Arrhythmia recurrence after atrial fibrillation ablation: Can magnetic resonance imaging identify gaps in atrial ablation lines? Journal of cardiovascular electrophysiology. 2008; 19:434–437. [PubMed: 18179530]
46. Koopmann M, Hong K, Kholmovski EG, Huang EC, Hu N, Ying J, Levenson R, Vijayakumar S, Dosdall DJ, Ranjan R, Kim D. Post-contrast myocardial t(1) and ecv disagree in a longitudinal canine study. NMR in biomedicine. 2014; 27:988–995. [PubMed: 24865566]
47. Fitts M, Breton E, Kholmovski EG, Dosdall DJ, Vijayakumar S, Hong KP, Ranjan R, Marrouche NF, Axel L, Kim D. Arrhythmia insensitive rapid cardiac t1 mapping pulse sequence. Magnetic resonance in medicine : official journal of the Society of Magnetic Resonance in Medicine / Society of Magnetic Resonance in Medicine. 2013; 70:1274–1282.
48. Dickfeld T, Kato R, Zviman M, Nazarian S, Dong J, Ashikaga H, Lardo AC, Berger RD, Calkins H, Halperin H. Characterization of acute and subacute radiofrequency ablation lesions with nonenhanced magnetic resonance imaging. Heart rhythm : the official journal of the Heart Rhythm Society. 2007; 4:208–214.
49. Schmidt EJ, Fung MM, Ciris PA, Song T, Shankaranarayanan A, Holmvang G, Gupta SN, Chaput M, Levine RA, Ruskin J, Reddy VY, D'Avila A, Aletras AH, Danik SB. Navigated dense strain imaging for post-radiofrequency ablation lesion assessment in the swine left atria. Europace : European pacing, arrhythmias, and cardiac electrophysiology : journal of the working groups on cardiac pacing, arrhythmias, and cardiac cellular electrophysiology of the European Society of Cardiology. 2014; 16:133–141.
50. Kuppahally SS, Akoum N, Burgon NS, Badger TJ, Kholmovski EG, Vijayakumar S, Rao SN, Blauer J, Fish EN, Dibella EV, Macleod RS, McGann C, Litwin SE, Marrouche NF. Left atrial strain and strain rate in patients with paroxysmal and persistent atrial fibrillation: Relationship to left atrial structural remodeling detected by delayed-enhancement mri. Circulation. Cardiovascular imaging. 2010; 3:231–239. [PubMed: 20133512]
51. Inoue YY, Alissa A, Khurram IM, Fukumoto K, Habibi M, Venkatesh BA, Zimmerman SL, Nazarian S, Berger RD, Calkins H, Lima JA, Ashikaga H. Quantitative tissue-tracking cardiac

magnetic resonance (cmr) of left atrial deformation and the risk of stroke in patients with atrial fibrillation. Journal of the American Heart Association. 2015:4.

52. Khurram IM, Maqbool F, Berger RD, Marine JE, Spragg DD, Ashikaga H, Zipunnikov V, Kass DA, Calkins H, Nazarian S, Zimmerman SL. Association between left atrial stiffness index and atrial fibrillation recurrence in patients undergoing left atrial ablation. Circulation. Arrhythmia and electrophysiology. 2016; 9:e003163.doi: 10.1161/CIRCEP.115.003163 [PubMed: 26966287]
53. Hsu SJ, Hubert JL, Smith SW, Trahey GE. Intracardiac echocardiography and acoustic radiation force impulse imaging of a dynamic ex vivo ovine heart model. Ultrasonic imaging. 2008; 30:63–77. [PubMed: 18939609]
54. Mende J, Wild J, Ulucay D, Radicke M, Kofahl AL, Weber B, Krieg R, Maier K. Acoustic radiation force contrast in mri: Detection of calcifications in tissue-mimicking phantoms. Medical physics. 2010; 37:6347–6356. [PubMed: 21302792]
55. Vejdani-Jahromi M, Nagle M, Jiang Y, Trahey GE, Wolf PD. A comparison of acoustic radiation force derived indices of cardiac function in the langendorff perfused rabbit heart. IEEE transactions on ultrasonics, ferroelectrics, and frequency control. 2016; 63(9):1288–95.
56. McGann C, Kholmovski E, Blauer J, Vijayakumar S, Haslam T, Cates J, DiBella E, Burgon N, Wilson B, Alexander A, Prastawa M, Daccarett M, Vergara G, Akoum N, Parker D, MacLeod R, Marrouche N. Dark regions of no-reflow on late gadolinium enhancement magnetic resonance imaging result in scar formation after atrial fibrillation ablation. Journal of the American College of Cardiology. 2011; 58:177–185. [PubMed: 21718914]
57. Beinart R, Khurram IM, Liu S, Yarmohammadi H, Halperin HR, Bluemke DA, Gai N, van der Geest RJ, Lima JA, Calkins H, Zimmerman SL, Nazarian S. Cardiac magnetic resonance t1 mapping of left atrial myocardium. Heart rhythm : the official journal of the Heart Rhythm Society. 2013; 10:1325–1331.
58. Ghugre NR, Pop M, Barry J, Connelly KA, Wright GA. Quantitative magnetic resonance imaging can distinguish remodeling mechanisms after acute myocardial infarction based on the severity of ischemic insult. Magnetic resonance in medicine : official journal of the Society of Magnetic Resonance in Medicine / Society of Magnetic Resonance in Medicine. 2013; 70:1095–1105.
59. Yang Y, Graham JJ, Connelly K, Foltz WD, Dick AJ, Wright GA. Mri manifestations of persistent microvascular obstruction and acute left ventricular remodeling in an experimental reperfused myocardial infarction. Quantitative imaging in medicine and surgery. 2012; 2:12–20. [PubMed: 23256056]
60. Grissom WA, Rieke V, Holbrook AB, Medan Y, Lustig M, Santos J, McConnell MV, Pauly KB. Hybrid referenceless and multibaseline subtraction mr thermometry for monitoring thermal therapies in moving organs. Medical physics. 2010; 37:5014–5026. [PubMed: 20964221]
61. Kolandaivelu A, Zviman MM, Castro V, Lardo AC, Berger RD, Halperin HR. Noninvasive assessment of tissue heating during cardiac radiofrequency ablation using mri thermography. Circulation. Arrhythmia and electrophysiology. 2010; 3:521–529. [PubMed: 20657028]
62. Hey S, Cernicanu A, de Senneville BD, Roujol S, Ries M, Jais P, Moonen CT, Quesson B. Towards optimized mr thermometry of the human heart at 3t. NMR in biomedicine. 2012; 25:35–43. [PubMed: 21732459]
63. Dong J, Dickfeld T, Dalal D, Cheema A, Vasamreddy CR, Henrikson CA, Marine JE, Halperin HR, Berger RD, Lima JA, Bluemke DA, Calkins H. Initial experience in the use of integrated electroanatomic mapping with three-dimensional mr/ct images to guide catheter ablation of atrial fibrillation. Journal of cardiovascular electrophysiology. 2006; 17:459–466. [PubMed: 16684014]
64. Dong J, Calkins H, Solomon SB, Lai S, Dalal D, Lardo AC, Brem E, Preiss A, Berger RD, Halperin H, Dickfeld T. Integrated electroanatomic mapping with three-dimensional computed tomographic images for real-time guided ablations. Circulation. 2006; 113:186–194. [PubMed: 16401772]
65. Armenean C, Perrin E, Armenean M, Beuf O, Pilleul F, Saint-Jalmes H. Rf-induced temperature elevation along metallic wires in clinical magnetic resonance imaging: Influence of diameter and length. Magnetic resonance in medicine : official journal of the Society of Magnetic Resonance in Medicine / Society of Magnetic Resonance in Medicine. 2004; 52:1200–1206.
66. Martin AJ, Baek B, Acevedo-Bolton G, Higashida RT, Comstock J, Saloner DA. Mr imaging during endovascular procedures: An evaluation of the potential for catheter heating. Magnetic

resonance in medicine : official journal of the Society of Magnetic Resonance in Medicine / Society of Magnetic Resonance in Medicine. 2009; 61:45–53.

67. Basar B, Rogers T, Ratnayaka K, Campbell-Washburn AE, Mazal JR, Schenke WH, Sonmez M, Faranesh AZ, Lederman RJ, Kocaturk O. Segmented nitinol guidewires with stiffness-matched connectors for cardiovascular magnetic resonance catheterization: Preserved mechanical performance and freedom from heating. Journal of cardiovascular magnetic resonance : official journal of the Society for Cardiovascular Magnetic Resonance. 2015; 17:105. [PubMed: 26620420]
68. Campbell-Washburn AE, Rogers T, Basar B, Sonmez M, Kocaturk O, Lederman RJ, Hansen MS, Faranesh AZ. Positive contrast spiral imaging for visualization of commercial nitinol guidewires with reduced heating. Journal of cardiovascular magnetic resonance : official journal of the Society for Cardiovascular Magnetic Resonance. 2015; 17:114. [PubMed: 26695490]
69. Tzifa A, Krombach GA, Kramer N, Kruger S, Schutte A, von Walter M, Schaeffter T, Qureshi S, Krasemann T, Rosenthal E, Schwartz CA, Varma G, Buhl A, Kohlmeier A, Bucker A, Gunther RW, Razavi R. Magnetic resonance-guided cardiac interventions using magnetic resonance-compatible devices: A preclinical study and first-in-man congenital interventions. Circulation. Cardiovascular interventions. 2010; 3:585–592. [PubMed: 21098745]
70. Tzifa A, Schaeffter T, Razavi R. Mr imaging-guided cardiovascular interventions in young children. Magnetic resonance imaging clinics of North America. 2012; 20:117–128. [PubMed: 22118596]
71. How astronomers may work. Science. 1886; 8:367.
72. Omary RA, Unal O, Koscielski DS, Frayne R, Korosec FR, Mistretta CA, Strother CM, Grist TM. Real-time mr imaging-guided passive catheter tracking with use of gadolinium-filled catheters. Journal of vascular and interventional radiology : JVIR. 2000; 11:1079–1085. [PubMed: 10997475]
73. Ocali O, Atalar E. Intravascular magnetic resonance imaging using a loopless catheter antenna. Magnetic resonance in medicine : official journal of the Society of Magnetic Resonance in Medicine / Society of Magnetic Resonance in Medicine. 1997; 37:112–118.
74. Yang X, Atalar E. Intravascular mr imaging-guided balloon angioplasty with an mr imaging guide wire: Feasibility study in rabbits. Radiology. 2000; 217:501–506. [PubMed: 11058652]
75. Susil RC, Yeung CJ, Halperin HR, Lardo AC, Atalar E. Multifunctional interventional devices for mri: A combined electrophysiology/mri catheter. Magnetic resonance in medicine : official journal of the Society of Magnetic Resonance in Medicine / Society of Magnetic Resonance in Medicine. 2002; 47:594–600.
76. Susil RC, Yeung CJ, Atalar E. Intravascular extended sensitivity (ives) mri antennas. Magnetic resonance in medicine : official journal of the Society of Magnetic Resonance in Medicine / Society of Magnetic Resonance in Medicine. 2003; 50:383–390.
77. Raval AN, Karmarkar PV, Guttman MA, Ozturk C, Desilva R, Aviles RJ, Wright VJ, Schenke WH, Atalar E, McVeigh ER, Lederman RJ. Real-time mri guided atrial septal puncture and balloon septostomy in swine. Catheterization and cardiovascular interventions : official journal of the Society for Cardiac Angiography & Interventions. 2006; 67:637–643. [PubMed: 16532499]
78. Arepally A, Karmarkar PV, Weiss C, Rodriguez ER, Lederman RJ, Atalar E. Magnetic resonance image-guided trans-septal puncture in a swine heart. Journal of magnetic resonance imaging : JMRI. 2005; 21:463–467. [PubMed: 15779027]
79. Nazarian S, Kolandaivelu A, Zviman MM, Meininger GR, Kato R, Susil RC, Roguin A, Dickfeld TL, Ashikaga H, Calkins H, Berger RD, Bluemke DA, Lardo AC, Halperin HR. Feasibility of real-time magnetic resonance imaging for catheter guidance in electrophysiology studies. Circulation. 2008; 118:223–229. [PubMed: 18574048]
80. Grothoff M, Piorkowski C, Eitel C, Gaspar T, Lehmkuhl L, Lucke C, Hoffmann J, Hildebrand L, Wedan S, Lloyd T, Sunnarborg D, Schnackenburg B, Hindricks G, Sommer P, Gutberlet M. Mr imaging-guided electrophysiological ablation studies in humans with passive catheter tracking: Initial results. Radiology. 2014; 271:695–702. [PubMed: 24484059]
81. AG, MP, AvdK, EN, SKW. Motion-robust mri through real-time motion tracking and retrospective super-resolution volume reconstruction. Annual International Conference of the IEEE Engineering

in Medicine and Biology Society IEEE Engineering in Medicine and Biology Society Conference; 2011; 2011. p. 5722-5725.

82. Dumoulin CL, Souza SP, Darrow RD. Real-time position monitoring of invasive devices using magnetic resonance. Magnetic resonance in medicine : official journal of the Society of Magnetic Resonance in Medicine / Society of Magnetic Resonance in Medicine. 1993; 29:411–415.
83. Leung DA, Debatin JF, Wildermuth S, McKinnon GC, Holtz D, Dumoulin CL, Darrow RD, Hofmann E, von Schulthess GK. Intravascular mr tracking catheter: Preliminary experimental evaluation. AJR. American journal of roentgenology. 1995; 164:1265–1270. [PubMed: 7717244]
84. Dumoulin CL, Mallozzi RP, Darrow RD, Schmidt EJ. Phase-field dithering for active catheter tracking. Magnetic resonance in medicine : official journal of the Society of Magnetic Resonance in Medicine / Society of Magnetic Resonance in Medicine. 2010; 63:1398–1403.
85. Dukkipati SR, Mallozzi R, Schmidt EJ, Holmvang G, d'Avila A, Guhde R, Darrow RD, Slavin G, Fung M, Malchano Z, Kampa G, Dando JD, McPherson C, Foo TK, Ruskin JN, Dumoulin CL, Reddy VY. Electroanatomic mapping of the left ventricle in a porcine model of chronic myocardial infarction with magnetic resonance-based catheter tracking. Circulation. 2008; 118:853–862. [PubMed: 18678773]
86. Schmidt EJ, Mallozzi RP, Thiagalingam A, Holmvang G, d'Avila A, Guhde R, Darrow R, Slavin GS, Fung MM, Dando J, Foley L, Dumoulin CL, Reddy VY. Electroanatomic mapping and radiofrequency ablation of porcine left atria and atrioventricular nodes using magnetic resonance catheter tracking. Circulation. Arrhythmia and electrophysiology. 2009; 2:695–704. [PubMed: 19841033]
87. Vernickel P, Schulz V, Weiss S, Gleich B. A safe transmission line for mri. IEEE transactions on biomedical engineering. 2005; 52:1094–1102. [PubMed: 15977738]
88. Eitel C, Hindricks G, Grothoff M, Gutberlet M, Sommer P. Catheter ablation guided by real-time mri. Current cardiology reports. 2014; 16:511. [PubMed: 24952899]
89. Harrison JL, Sohns C, Linton NW, Karim R, Williams SE, Rhode KS, Gill J, Cooklin M, Rinaldi CA, Wright M, Schaeffter T, Razavi RS, O\Neill MD. Repeat left atrial catheter ablation: Cardiac magnetic resonance prediction of endocardial voltage and gaps in ablation lesion sets. Circulation. Arrhythmia and electrophysiology. 2015; 8(2):270–8. [PubMed: 25593109]
90. Schmidt EJ, Tse ZT, Reichlin TR, Michaud GF, Watkins RD, Butts-Pauly K, Kwong RY, Stevenson W, Schweitzer J, Byrd I, Dumoulin CL. Voltage-based device tracking in a 1.5 tesla mri during imaging: Initial validation in swine models. Magnetic resonance in medicine : official journal of the Society of Magnetic Resonance in Medicine / Society of Magnetic Resonance in Medicine. 2014; 71:1197–1209.
91. Mandal K, Parent F, Martel S, Kashyap R, Kadoury S. Vessel-based registration of an optical shape sensing catheter for mr navigation. International journal of computer assisted radiology and surgery. 2016; 1(6):1025–34.
92. Michaud, GF., Steigner, M., Schmidt, EJ., Houtaling, CST., Jerosch-Herold, M., Epstein, L., Kwong, RY. Preliminary results from 3t-mri during radiofrequency catheter ablation for atrial fibrillation. Heart rhythm : the official journal of the Heart Rhythm Society; Proceedings of Heart Rhythm Annual meeting; 2012; 2012. p. IA02-09.

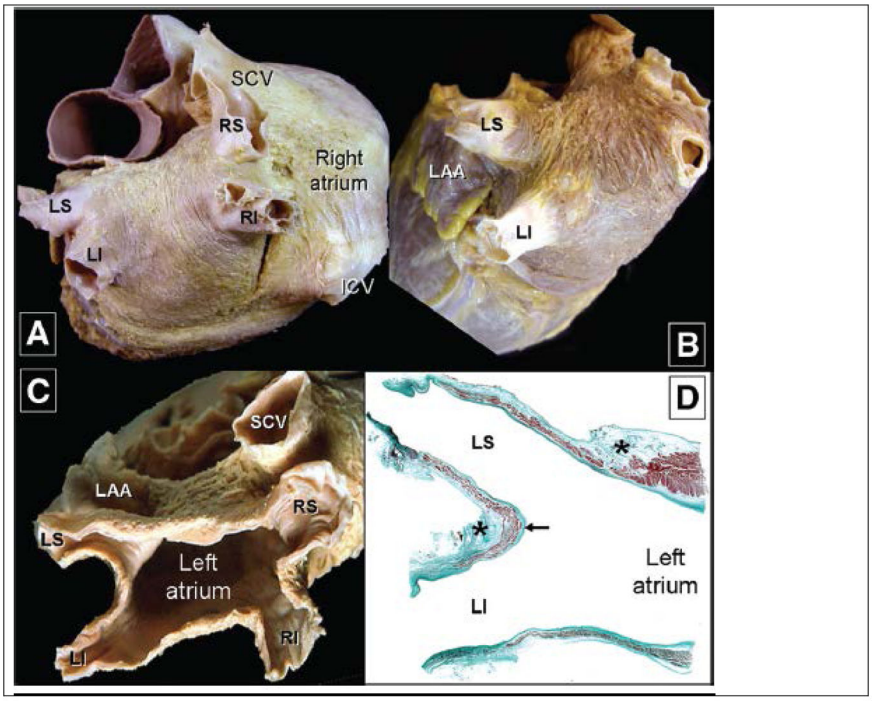

Figure 1.

Anatomic views of the Left atrium from a heart in which the epicardium has been removed. Parts A–C show classic views of the left atrium and the associated pulmonary veins. Part D, a stained thin section, shows the muscle sleeves entering the pulmonary veins, with the stars showing location of nerves in the surrounding fat-pads. (After Ho S.Y. et al. Circulation Arrhythmia & Electrophysiology 2012[21], with permission)

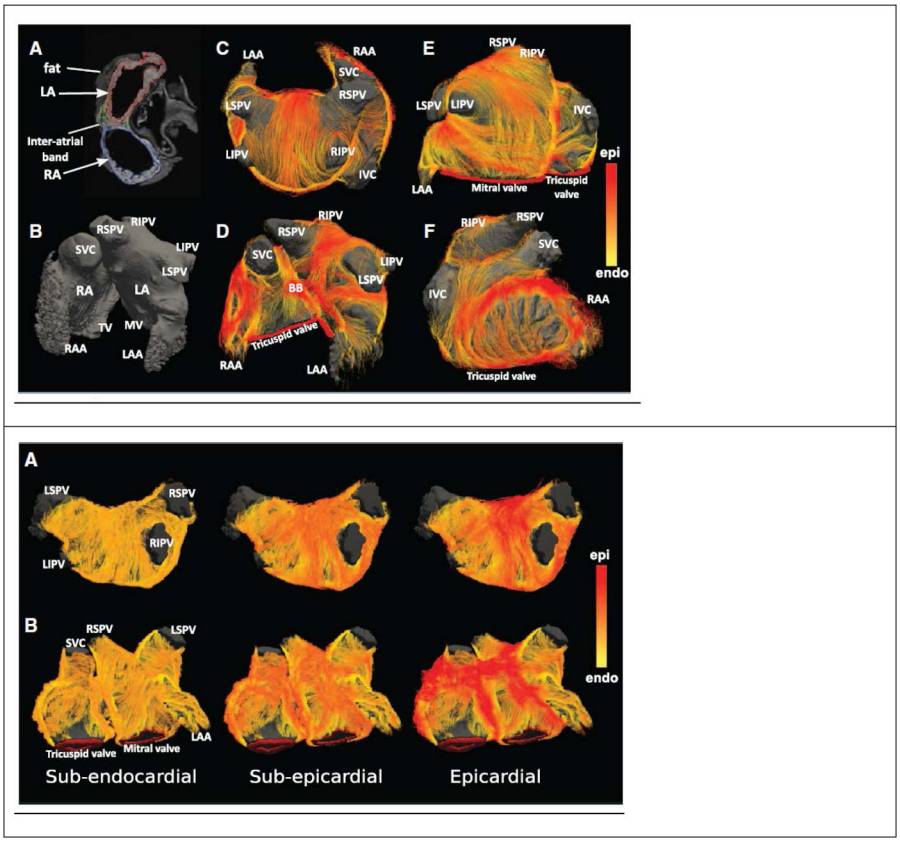

Figure 2.

Fiber tractography of normal human atria, obtained from diffusion-weighted MRI imaging of ex-vivo samples. (Top) Atrial geometry. Left column (A, B) shows standard T1-weighted MRI images of the anatomy. Middle column (C, D) External surface view of the fiber tracts. Right column (E, F) anterior view of atrium. (Bottom) Changes in fiber tract orientation with depth in the left atrial wall of a single subject. Color code on right measures the similarity to the fiber tract direction on the epicardial surface. (After Pashakhanloo F et al., Circulation Arrhythmia & Electrophysiology 2016[25], with permission)

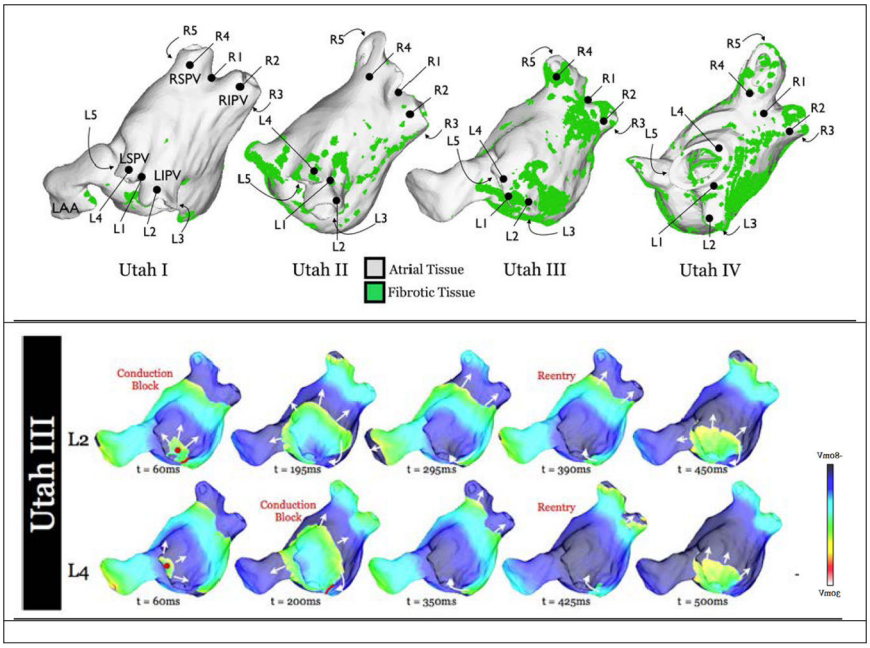

Figure 3.

Distribution of Fibrotic tissue, as observed with navigated LGE MRI imaging. Top: The University of Utah group headed by Dr. N. Marouche, has separated AF patients into groups termed Utah I-Utah IV, according to the distribution of fibrotic tissue in the atrium. Different density and distribution of fibrotic tissue can sustain different forms of fibrillatory rotors. Bottom: Examples of propagation of electrical fibrillatory waves from two different foci (L2, L4) in the PV-atrium junction for a Utah III type patient. (After McDowell K.S. et al. Plos 1 2015[34], with permission)

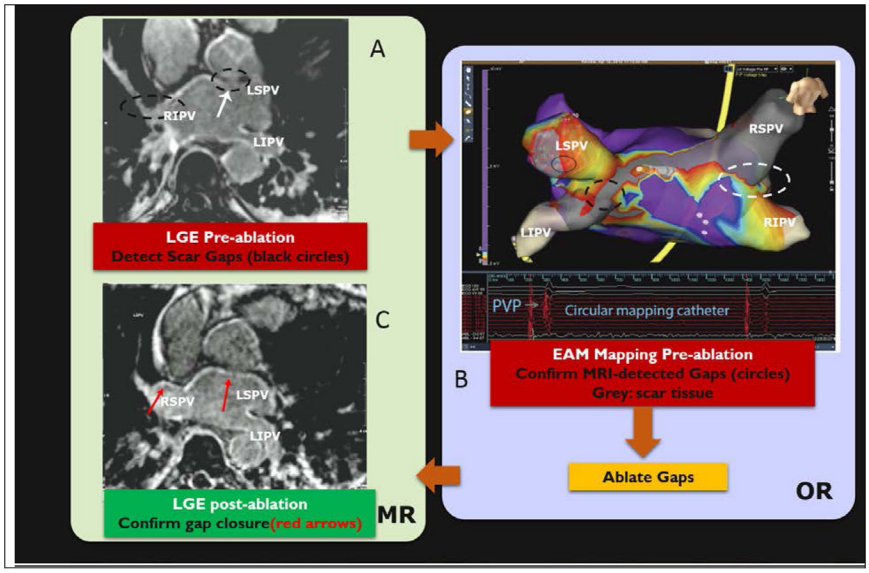

Figure 4.

Human procedure for repair of atrial fibrillation recurrence. Procedure involved (A) imaging the patient with LGE and MRA in an MRI prior to the intervention, in order to detect gaps in ablation lesions in the left atrium [lack of hyper-intense signal on the atrial wall], (B) patient transfer to a conventional EP lab where the MRI images were registered to a commercial Electro-anatomic (EAM) map and then the gaps were confirmed by navigating catheters to these locations, measuring wall voltages to establish that the MRI-seen gaps were actually there, and ablating the gaps with RF, and (C) transfer of the patient back to the MRI suite for a post-operative LGE, which confirmed that the gaps were indeed closed. AF has not recurred in any of the 7 patients studied in this protocol. (After Michaud G. F. et al, Proceedings of Heart Rhythm society, 2012[92]).

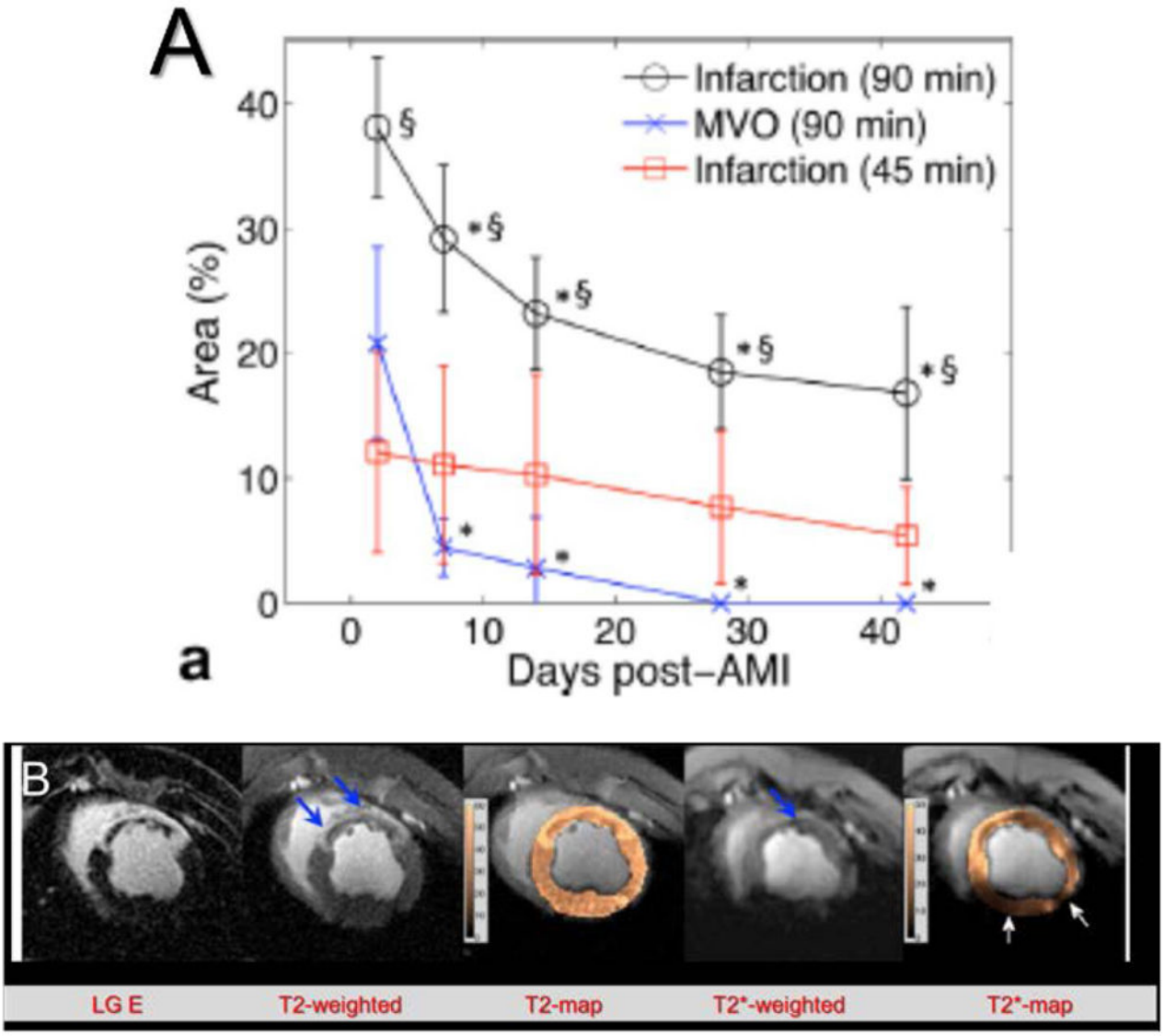

Figure 5.

Changes in a left ventricular infarct over time, as seen with different sequences. Infarct was created by a 45- or 90-minute coronary occlusion. (A) Graph showing the reduction in size of the apparent infarct over time. Note that the true necrotic region (Infarction 45 min, in red) does not substantially decrease over time. (B) Several imaging sequences performed on a 90-minute occlusion infarct. LGE, T2-weighted, and T2 map show both the infarct core and the surrounding edema (thick blue arrows), while T2*-weighted image and T2* map show true infarct core as dark (thin blue arrow) region. (After Ghugre N. R. et al., Magn. Res. Med. 2013[58], with permission)

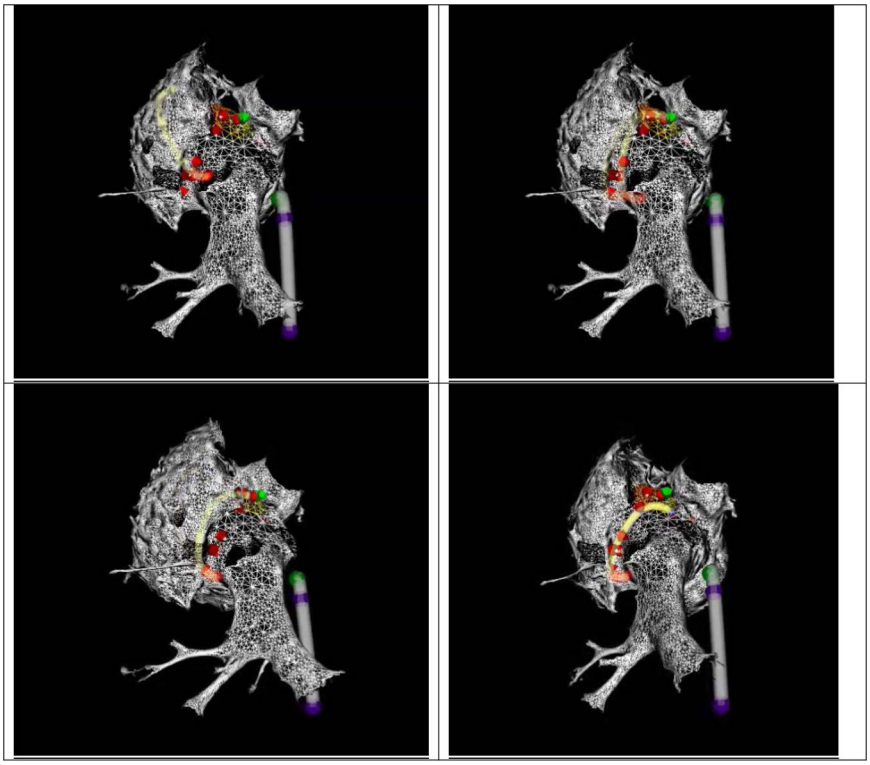

Figure 6.

Four frames from a Radio-Frequency thermal ablation of a swine left atrium using MR-Tracking guidance. Two devices are tracked simultaneously; a deflectable sheath (grey shaft, blue tracked locations on shaft) and an ablation catheter (yellow shaft, red tracked locations on shaft). The atrial geometry was obtained from a navigated ECG-gated CE-MRA scan. The ablation catheter is ablating the left-atrial pulmonary-vein ostium in a point-by-point method, with the ablation points defined by red arrows. (After Schmidt E. J. et al., Circulation Arrhythmia and Electrophysiology 2009[86], with permission)

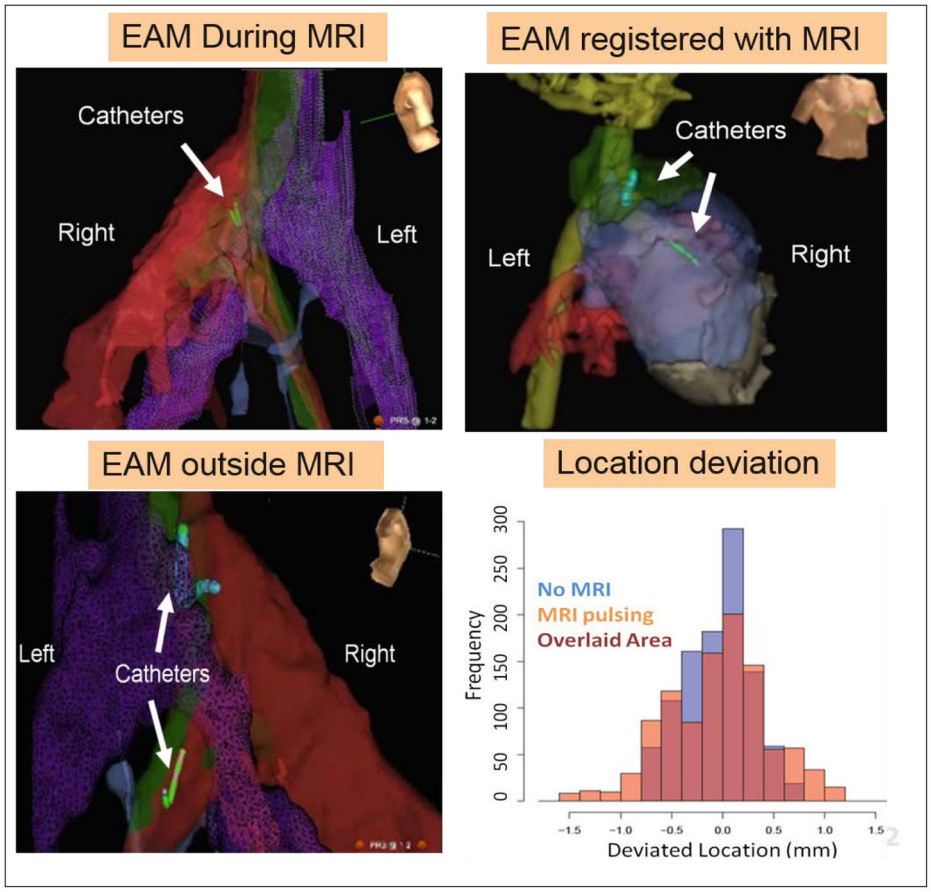

Figure 7.

Voltage Device Tracking in a swine. Three VDT MRI-compatible catheter were simultaneously tracked. (A) Tracking and collecting Electro-Anatomic (EAM) maps inside the MRI. (B). VDT tracking can be transferred to the MRI frame of reference, if MRI anatomic images are acquired, displayed navigation on MRI roadmaps. (C) After the swine was moved out of the MRI, navigation was continued without requiring registration. (D) Graph showing the small difference in location between VDT tracking performed inside the MRI during (MRI pulsing) or in the absence of imaging (No MRI). (After Schmidt E.J. et al., Mag Res Med 2014[90], with permission)